Heliyon 10 (2024) e40374

Contents lists available at ScienceDirect

Heliyon

journal homepage: www.cell.com/heliyon

Research article

Development and characterization of gastro-floating sustained-release granules for enhanced bioavailability of patchouli oil

Chen Liu [a,b,1], Yanan Wu [b,1], Yeli Zou [b], Jiao Wang [c], Boli Li [b], Yanni Ma [a], Xia Zhang [b], Wenping Wang [c,*]

[a] General Hospital of Ningxia Medical University, Yinchuan, Ningxia, 750004, China
[b] College of Pharmacy, Ningxia Medical University, Yinchuan, 750004, China
[c] College of Chinese Materia Medica, Yunnan University of Chinese Medicine, Kunming, Yunnan, 650500, China

ARTICLE INFO

Keywords:
Patchouli oil
Gastroretentive granules
Bioavailability
Sustained release
Colloidal silicon dioxide
Adsorption

ABSTRACT

Patchouli oil (PO), extracted from *Pogostemon cablin* Benth., a prominent aromatic plant of the Lamiaceae family, has shown considerable protective effects against gastrointestinal infections, particularly those induced by *Helicobacter pylori*. This study aimed to develop a gastro-floating multi-unit system for PO to enhance its gastric retention and oral bioavailability.
Methods: The oil-laden granules were prepared using colloidal silicon dioxide (CSD) for oil adsorption and to provide buoyancy, along with ethyl cellulose (EC) and hydroxypropyl methyl cellulose (HPMC) to form a sustained-release matrix. The CSD exhibited favorable characteristics for oil adsorption and floating. Compatibility between PO and CSD was affirmed through DSC thermograms and FTIR spectra. The obtained granules demonstrated a sustained release profile, achieving over 90 % release within 10 h without an initial burst. After oral administration, the granules were observed to remain in the gastric region of rats for over 7 h. The bioavailability of patchouli alcohol from the optimized granules was significantly higher than that from of the PO-loaded powders. The gastro-floating sustained-release granules, based on a CSD/EC/HPMC matrix, offer a simple yet effective strategy to improve the delivery efficacy of PO against *Helicobacter pylori* infections in the gastric region.

1. Introduction

Pogostemon cablin (Blanco) Benth., commonly known as Patchouli, is a famous aromatic plant within the Lamiaceae family, predominantly cultivated in tropical Asian regions for its essential oil production [1]. Patchouli oil (PO) serves as a versatile ingredient across the fragrance and food industries. In traditional Chinese medicine (TCM), it is recognized as "Guanghuoxiang" and has been utilized for treating gastrointestinal disorders since the East Han dynasty [2]. Its therapeutic use is also reflected in modern pharmaceuticals such as Huoxiang Zhengqi oral solutions and Baoji pills. Scientific literature documents the multifaceted therapeutic properties of Patchouli extracts, including antimicrobial, anti-inflammatory, antioxidant, and antidepressant effects. PO has

* Corresponding author.
E-mail address: wangwenping@ynucm.edu.cn (W. Wang).
[1] They contributed equally to this work as the co-first authors.

https://doi.org/10.1016/j.heliyon.2024.e40374
Received 2 July 2024; Received in revised form 7 September 2024; Accepted 12 November 2024
Available online 13 November 2024
2405-8440/© 2024 Published by Elsevier Ltd. This is an open access article under the CC BY-NC-ND license (http://creativecommons.org/licenses/by-nc-nd/4.0/).

demonstrated protective effects against *Helicobacter pylori* (*H. pylori*)-induced gastrointestinal infections and ulcers [3]. A key constituent, Patchouli alcohol (PA), inhibits urease specifically [4] and enhances defense mechanisms against intracellular *H. pylori* by promoting miR-30b/c-mediated xenophagy [5]. Another significant component, Patchouli ketone (PK), also exhibits robust antimicrobial activity [6].

H. pylori is a prevalent global infection, closely associated with gastric cancer, peptic ulcers, and atrophic gastritis [7]. Classified as a Group 1 carcinogen by the World Health Organization since 1994, the rise of antibiotic resistance has complicated *H. pylori* eradication, challenging even the standard triple therapy of a proton-pump inhibitor, amoxicillin, and clarithromycin [8]. The safety of these treatments is also under scrutiny [9]. There is, therefore, an urgent need for alternative therapies, particularly those from natural sources. Medicinal plant essential oils, including PO, are emerging as promising candidates for managing *H. pylori* infections due to their lower side effects and established antimicrobial activity [10–12].

Given *H. pylori*'s residence at the mucosalepithelial cell interface of the gastric mucus layer, gastro-retentive drug delivery systems (GRDDS) are strategic for enhancing the therapeutic efficacy of antibacterial drugs in the stomach [13]. Various systems have been designed for sustained and localized release of active ingredients in the gastric region, including floating, mucoadhesive, and swellable devices [14]. Floating dosage forms, particularly in multiple units (e.g., granules, beads, microspheres, pellets, and mini-tablets), have shown the most promise. These buoyant systems achieve a lower bulk density than gastric fluid (1.004–1.010 g mL^{-1}) through lightweight-carrier materials, hollow structures, or gas-generating agents [15]. Among various materials, the low density and high porosity of CSD [16] allows it to serve as an effective adsorbent carrier for oils and a buoyant agent in the formulation of gastro-retentive drug delivery systems, enhancing the performance of such systems by prolonging the residence time of the dosage form in the gastric environment.

This study presents an integrated formulation strategy for enhancing the gastric delivery of essential oils. Specifically, we utilized CSD for PO adsorption and buoyancy, and a combination of ethyl cellulose (EC) and hydroxypropyl methyl cellulose (HPMC) to control the drug release profile meticulously. The primary objectives were to fabricate gastro-floating granules and to access their *in vitro* and *in vivo* performance concerning gastro-retention capabilities and the modification of drug delivery kinetics.

2. Materials and methods

2.1. Materials

High-purity PO and PK, both exceeding 98 % purity, were sourced from Jingzhu Biotech Co., Ltd in Nanjing, China. PA was procured from the National Institutes for Food and Drug Control in Beijing, China, and isoalantolactone was acquired from Alfa Biotech Co., Ltd in Chengdu, China. As adsorbents and matrix materials, we utilized Colloidal silicon dioxide (CSD, AEROSIL® R972 Pharm), Microcrystalline cellulose (MCC, Avicel® PH102), Ethylcellulose (EC), and Hydroxypropyl methyl cellulose (HPMC K15MCR), all of which were supplied by Sinopharm Chemical Reagent Co., Ltd in Shanghai, China. Starch was purchased from Youpuhui Pharmaceutical Co., Ltd in Shenzhen, China. All additional reagents used were of analytical grade. For the preparation of solutions in this study, we employed purified or ultra-purified water provided by Milli-Q (Millipore, USA).

2.2. Patchouli oil adsorption assessment

We weighed out equal parts of PO and various excipients, which were then mixed in a mortar and ground for 5 min to form a uniform mixture. A panel of four commonly utilized excipients was evaluated fro their oil-adsorption capabilities, including calcium carbonate, starch, MCC, and CSD. The goal was to access and compare their relative effectiveness as adsorbents for PO.

2.3. Fabrication of sustained-release granules

PO, representing 15 % of the total weight, was mixed with either CSD or MCC at a 35 % ratio using a mortar and pestle. Then, EC and HPMC were added at a 22.5 % and 27.5 % weight fractions, respectively, and the mixture was thoroughly integrated. Ethanol served as a wetting agent to prepare a malleable mass, which underwent extrusion at 25 Hz and spherization at 27 Hz for 10 min using a WL350 centrifugal pellet machine (Wenzhou Pharmaceutical Machinery Factory, Wenzhou, China). The resulting granules were sealed and refrigerated for further analysis.

2.4. Assessment of in vitro buoyancy

For the oil-loaded powders, a 0.5 g sample was accurately weighed and placed into a beaker with 250 mL of 0.1M HCl solution. The mixture was manually stirred for 1 min with a glass rod to ensure uniform dispersion, and the dispersion state of the powder was then carefully observed.

For the oil-loaded granules, a set quantity was placed in 250 mL of 0.1M HCl within a water bath at a temperature of 37 ± 0.5 °C. The mixture was continuously stirred for 8 h to mimic gastric conditions. The floating granules were collected, counted, and the floating percentage (F, %) was calculated based on these observations.

2.5. Characterization of patchouli Oil-CSD interactions

To determine the nature of the interactions between PO and CSD, we employed Differential Scanning Calorimetry (DSC) and Fourier-Transform Infrared (FTIR) spectroscopy. The DSC measurements were conducted using an X'pert PRO DSC instrument (Spectris, Holland), where the samples underwent a temperature ramp of 10 °C per minute from −80 °C to 500 °C. Nitrogen served as the purge gas, with Al_2O_3 as the reference material. The FTIR spectra of the pure PO, CSD, and their mixture were recorded using a TENSOR 37 FTIR spectrophotometer (Bruker, Germany) across a wavenumber range of 400–4000 cm^{-1}.

2.6. In vitro drug release analysis

Drug release kinetics of the oil-loaded granules were evaluated using an RCZ-8M dissolution apparatus (paddle method, Tianda Tianfa Technology Co., Ltd., Tianjin, China). The tests were conducted in a 900 mL volume of 0.1 M HCl solution maintained at 37 °C and stirred at a rate of 50 revolutions per minute (rpm). At specified intervals, 5 mL aliquots were removed, and an equal volume of pre-warmed medium was immediately added to maintain sink conditions. For comparative analysis, the oil-MCC mixture was subjected to the same procedure. The withdrawn samples were passed through 0.22 μm syringe filters to remove particulates and subsequently analyzed using a validated High-Performance Liquid Chromatography (HPLC) method. Each measurement was performed in triplicate to ensure reliability, with results expressed as the mean ± standard deviation.

To elucidate the release behavior and underlying mechanisms, the drug release data were subjected to curve fitting using a suite of kinetic models, including first-order, zero-order, Korsmayer-Peppas, and Higuchi models. The model demonstrating the highest correlation coefficient (R^2) was identified as the optimal fit for the release profile, thereby providing insights into the dominant release mechanism at play [17].

2.7. Assessment of in vivo gastro-retention

The gastro-retentive capacity of the sustained-release granules was accessed *in vivo* using Sprague-Dawley (SD) rats, employing X-ray imaging [18,19]. Barium sulfate was used in place of PO was uniformed mixed with the excipients, then granulated using the method previously described. The rats were orally administered the $BaSO_4$-laden granules and imaged at 0, 0.5, 1, 1.5, 2, 4, and 6 h post-administration using the DigiEye 280 medical radiography system (Mindray, Shenzhen, China). After a 7-h study period, the rats were euthanized, and the gastric contents were examined to verify granule retention.

2.8. In vivo pharmacokinetic study

Male SD rats, weighing approximately 210 ± 10 g and certified by the Animal Experimental Center of Ningxia Medical University (SYXK, Ning 2015-0002), were used for the pharmacokinetic study. The study adhered to the "Guidelines for the Care and Use of Laboratory Animals" and was approved by the Animal Experimental Committee of Ningxia Medical University (No. 2016-046). Rats were fasted overnight with water access prior to dosing. PO was mixed with MCC at a 1:2 wt ratio to prepare the oil-loaded powder. This powder and the equivalent granules were encapsulated for oral administration. Rats were randomly divided into two groups and given either the oil-loaded powder or granules at a dosage of 60 mg/kg body weight. Blood samples (0.3 mL) were collected at predetermined time points from 5 min to 72 h post-administration via the orbital sinus. Plasma was separated by centrifugation at

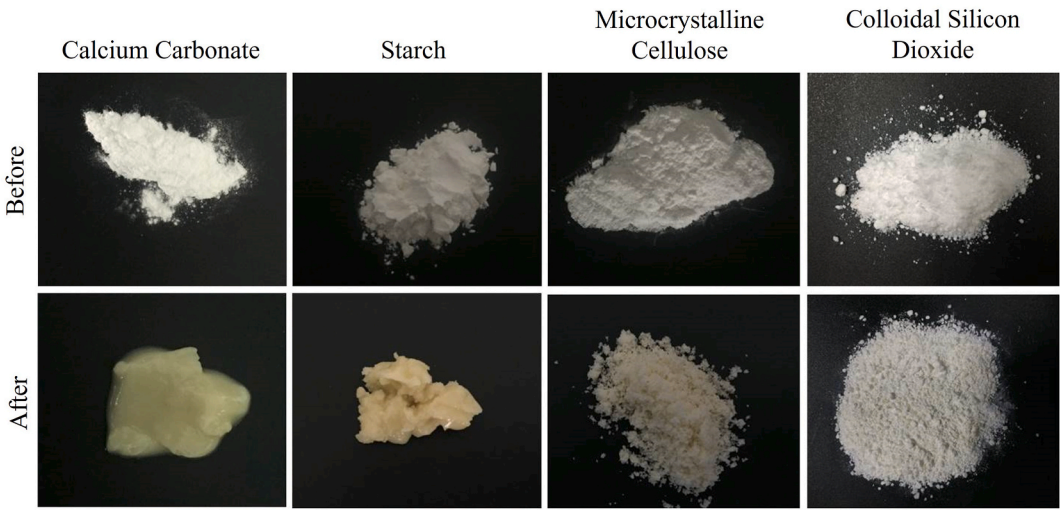

Fig. 1. Appearance of different adsorbents before (upper) and after (lower) mixed with Patchouli Oil.

4000 rpm for 10 min and processed with an internal standard and ethyl acetate, followed by centrifugation at 12000 rpm for 10 min to obtain the supernatant. After evaporated under a nitrogen stream and reconstitution in methanol, 1 μL of the supernatant was analyzed using a gas chromatography (GC) system.

2.9. Statistical analysis

Data analysis was conducted using the Statistical Analysis System (SAS) software, version 9.4. Descriptive statistics were calculated for all pharmacokinetic parameters. Group comparisons were performed using one-way analysis of variance (ANOVA), followed by Tukey's Honestly Significant Difference (HSD) post-hoc test for multiple comparisons. Statistical significance was set at a p-value less than 0.05.

3. Results

3.1. Patchouli oil adsorption

In our study, we evaluated the efficacy of four excipients — calcium carbonate, starch, MCC, and CSD — as adsorbents for PO at a 1:1 wt ratio of powder to oil. Each excipient, presented as a fine white or off-white powder, was compared for its ability to absorb PO, a transparent yellowish-brown liquid. After thorough grinding, the mixtures exhibited varying appearances (as depicted in Fig. 1). Specifically, the mixtures with calcium carbonate or starch resulted in a pale yellowish paste, indicative of an excess oil phase. In contrast, the mixtures with MCC or CSD maintained an off-white hue, with CSD showing enhanced dispersibility and flow characteristics. These results led to the selection of MCC and CSD as the most effective adsorbents for PO, which were then utilized in the preparation of granules for further analysis.

Colloidal silicon dioxide, an amorphous inorganic aerogel of highly pure silicon dioxide, is recogonized as a nanomaterial with an average particle size between 30 and 40 nm [20]. Its diverse applications including serving as an absorbent carrier for substances and as a gelator that forms a network of aggregates [21,22]. Lunter et al. demonstrated that mesoporous silica particles can adsorb 2.3–3.2 g of refined castor oil per gram of silica, which is dependent on the silica's pore volume and particle size [23]. This characteristic endows CSD with the unique ability to absorb substantial quantities of oils without compromising its free-flowing powder properties, providing significant advantages for the formulation of essential oils in solid dosage forms. The application of CSD in the current study aligns with previous studies, showcasing its potential in utilizing the drug loading ability of essential oils like PO.

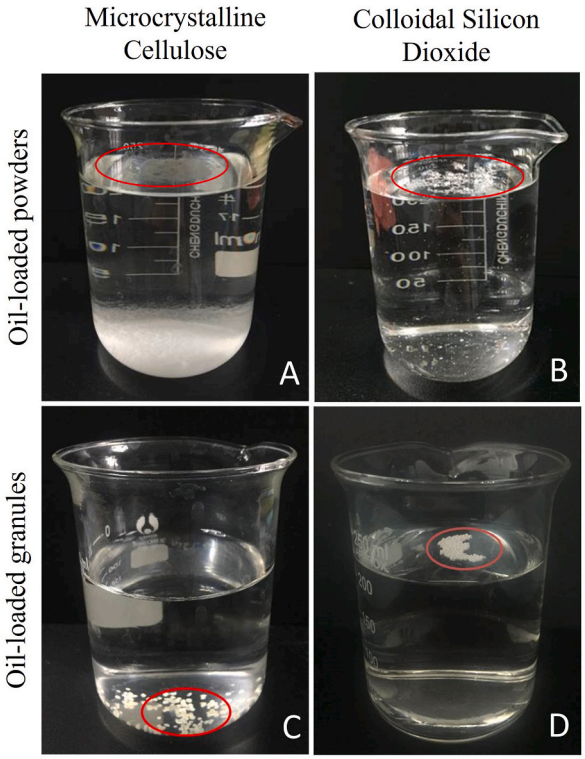

Fig. 2. *In vitro* floating performance of oil-loaded powders (A,B) and granules (C,D) of MCC (A,C) or CSD (B,D).

3.2. In vitro buoyancy assessment

We examined the buoyancy of oil-loaded powders and granules, with the findings presented in Fig. 2.

Upon gentle agitation, the oil-laden MCC powder rapidly separated into two distinct layers (Fig. 2A): a minor portion with oil droplets that stay afloat on the surface, and the bulk of the powder that sank to the bottom of the beaker. In contrast, the CSD-adsorbed granules mostly stayed buoyant without visible oil droplets (Fig. 2B). This finding suggests that MCC lacks inherent buoyancy necessary for sustained floating and tends to undergo swift phase separation from the oil in aqueous medium. Conversely, CSD, even when loaded with oil, demonstrated superior floating capabilities and efficient maintained the oil within the aqueous solution.

3.3. Characterization of interactions between PO and CSD

Fig. 3 presents the DSC thermograms and FTIR spectra for PO, CSD, and their composite powder. The DSC thermograms indicated an endothermic transition for PO at around 250 °C, a characteristic that was maintained in the oil-loaded CSD. The lack of distinct peaks in the thermogram of pure CSD is due to its amorphous nature [24]. The reduced peak intensity of PO in the CSD mixture is likely due to the excipient's dilution effect.

In the FTIR spectrum of PO, the significant peak at 3500 cm^{-1} is corresponds to the stretching vibrations of the hydroxyl (O-H) functional groups. The presence of C-H bonds is indicated by the bands ranging from 3000 cm^{-1} to 2850 cm^{-1}. Additionally, the bands detected at 1460 cm^{-1} and 1380 cm^{-1} correspond to the bending vibrations of the methyl (CH_3) and methylene (CH_2) groups within the molecular ring structures. The FTIR spectrum of PO closely resembles that of PA as reported in a previous study [25], a similarity expected given that PA is a principal constituent of the oil, with other components sharing a molecular structure akin to PA. The CSD's FTIR spectrum exhibited characteristic bands at 540 cm^{-1} (asymmetrical stretching of Si-O bonds), 1015 cm^{-1} (asymmetrical stretching of Si-O-Si bonds), 1270 cm^{-1}, and 760 cm^{-1} (asymmetrical stretching of Si-C bonds) [26]. These distinctive peaks were also observed in the oil-CSD mixture spectrum, with no new peaks indicating the absence of chemical interactions or physical changes following adsorption.

These findings confirmed the compatibility of PO with CSD, suggesting that CSD can serve as an effective adsorbent and floating agent without altering the chemical structure of the oil, which is crucial for the development of stable and effective drug delivery systems.

3.4. In vitro dissolution profiles

The *in vitro* dissolution data, as illustrated in Fig. 4, elucidate the release kinetics of the MCC powder and the gastro-floating granules containing PO. The MCC powder, upon adsorption of the oil, displayed a rapid release profile, with over 55 % of the drug being released within the initial 15 min, and nearly complete release, reaching approximately 90 % within 1 h. This swift separation is consistent with the observations from the floating tests. In contrast, the granules exhibited a sustained release pattern, characterized by an initial lag phase of about 15 min, followed by a gradual ascent to 90 % release over a 10-h period, absent of an initial burst. This behavior underscores the excellent controlled-release characteristics of the granules.

The incorporation of HPMC in the matrix typically triggers the formation of a viscous gel layer upon contact with the dissolution medium, acting as a barrier that retards the drug's migration to the release medium [27]. This mechanism can often lead to an initial

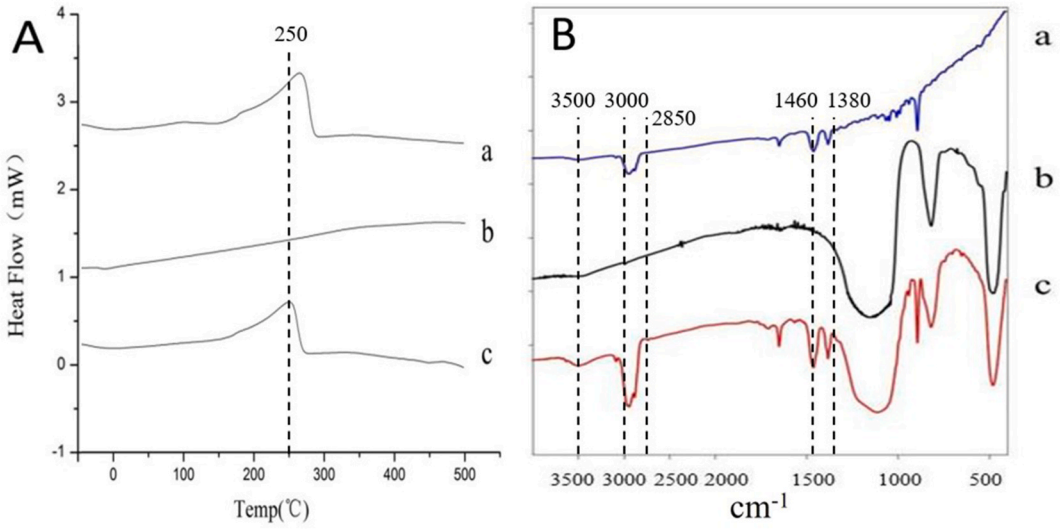

Fig. 3. DSC thermograms (A) and FTIR spectra (B) of (a) patchouli oil, (b) CSD and (c) their mixture.

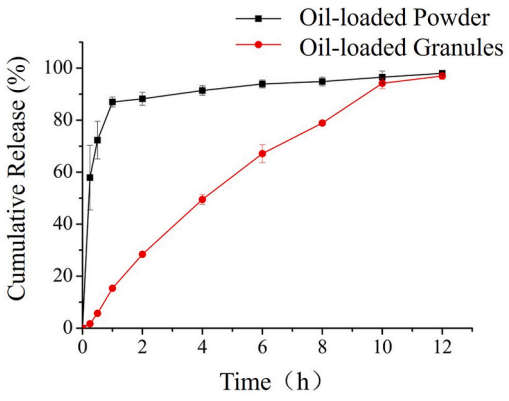

Fig. 4. *In vitro* drug release profiles of MCC powder and gastro floating CSD granules loaded with patchouli oil (n = 3).

burst release when utilizing a pure HPMC matrix [28]. To counteract this, EC, a hydrophobic excipient, was incorporated to modulate the drug release kinetics, particularly to control the burst release [29,30]. Furthermore, the adsorptive nature of CSD enables it to bind oil within its internal surface, requiring the drug molecule to traverse the silica's pore network before entering the dissolution medium. This interaction may function as a rate-limiting step in the drug release process, providing an additional layer of control over the release behavior [23,31]. Thus, the combined effect of EC, HPMC, and CSD within the granules effectively governed the dissolution profile of the PO-loaded system.

To elucidate the release kinetics of PK from the gastro-floating granules, a variety of mathematical models were applied. As detailed in Table 1, each model provided a strong fit, with R^2 all surpassing the threshold of 0.95. The Higuchi model was particularly prominent, exhibiting the highest R^2 value of 0.9962, indicating its optimal conformity to the experimental data.

The Korsmeyer-Peppas model yielded a diffusion exponent (n) of 0.9946, a figure exceeding 0.89. This is indicative of a super Case II transport mechanism, typical of non-Fickian release mechanism [32]. This suggests that the principal mechanism governing drug release from the granules is diffusion-controlled [33]. In this mechanism, the dissolution medium initially infiltrates the granules, dissolving the encapsulated drug, which subsequently diffuses outward. Throughout this process, the relaxation of the polymer matrix exerts a pivotal influence on the diffusion of the drug molecules [34].

3.5. *In vivo buoyancy and gastrointestinal distribution*

Fig. 5 depicts the gastrointestinal tract (GIT) distribution of granules following oral administration in rats. The granules' transit through the GIT was clearly observable; the initial radiograph showed the rat's skeletal framework without any visible contents. After administration, the granules were quickly located in the stomach's upper region and were still visible in the gastric area for up to 6 h, albeit with changes in position and distribution.

Further validation of the granules' gastric retention was achieved by sacrificing and dissecting the rats, as shown in Fig. 6. Many white particles, signifying the retained granules, were apparent in the stomach, with some shape distortion possibly due to erosion effects *in vivo*. Together, the X-ray images and the analysis of gastric contents confirmed that the granules sustained buoyancy in the abdominal region for over 7 h post-administration.

3.6. *Pharmacokinetic evaluation in vivo*

Fig. 7 illustrates the comparative plasma concentration-time profiles of PO when administrated as both powder and granule formulations. A detailed overview of the pharmacokinetic parameters is presented in Table 2. Statistically significant differences were observed between the two formulations in terms of area under the curve (AUC), time to reach maximum concentration (T_{max}), and maximum concentration (C_{max}). Notably, the granule formulation demonstrated a lower C_{max} but a significantly extended T_{max} for both PA and PK, indicative of a sustained release profile *in vivo*. The mean residence time (MRT) was also slightly prolonged for the granules, reinforcing the formulation's sustained-release characteristics. Importantly, the AUC values for both PA and PK were considerably higher for the granules, suggesting an enhancement in oral bioavailability.

Table 1
The curve fitting of drug release data from oil-loaded granules.

Models	Equations	Correlation coefficients(R^2)	Diffusion index(n)
Zero-order	y = 8.4131x + 7.7461	0.9623	–
First-order	y = −0.2828x + 4.8396	0.9506	–
Higuchi	y = 34.0920× - 17.7440	0.9962	–
Korsmeyer–Peppas	y = 0.9946x + 2.3716	0.9663	0.9946

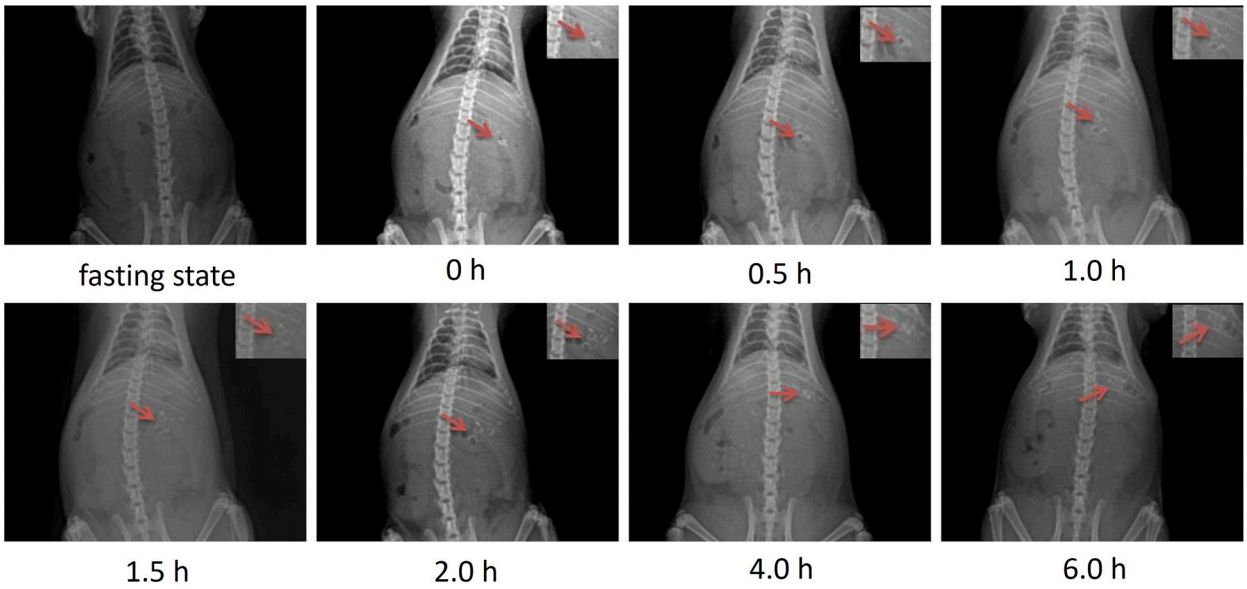

Fig. 5. Appearance of rat stomach before (A) and after (B) gastric dissection after oral administration for 7 h.

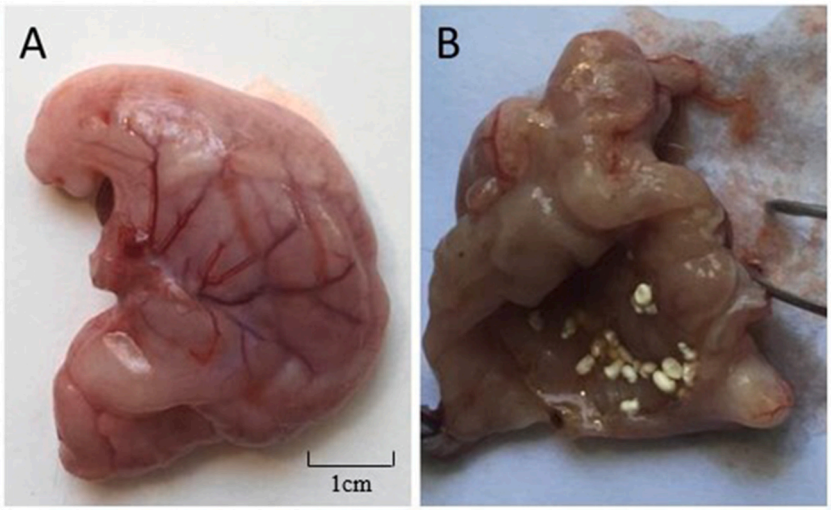

Fig. 6. Radiographic images of BaSO4-loaded granules in rat stomach before (fasting state) and after oral administration.

A comparison of the *in vivo* performance of PA and PK revealed similar plasma concentration-time curves, suggesting a consistent influence of the granules on the pharmacokinetics of these components. The comparable MRT, half-life ($t_{1/2}$), and T_{max} values for PA and PK imply a similar systematic exposure following oral administration. However, PK exhibited markedly higher C_{max} and AUC values compared to PA, pointing to its superior oral absorption, despite being present in lower concentration within the oil. This aligns with previous studies that have reported high bioavailability for PK after oral ingestion [35].

Within the composition of PO, PA constitutes over 26 % by weight and is recognized as the primary constituent responsible for the oil's characteristic quality and aroma. A previous study by Zhang et al. investigated the pharmacokinetics of PA following a single oral dose in rats [35]. Their findings indicated that both C_{max} and AUC were higher for pure PA than for equivalent doses of PO. Interestingly, T_{max} values were significantly higher in the PO group, suggesting that other components in the oil may influence the absorption kinetics of PA.

4. Conclusions

This study presents the development of an innovative gastro-floating sustained-release granule system designed for the delivery of PO. Our results demonstrate that the incorporation of CSD significantly improved the granules' buoyancy and gastric retention, which

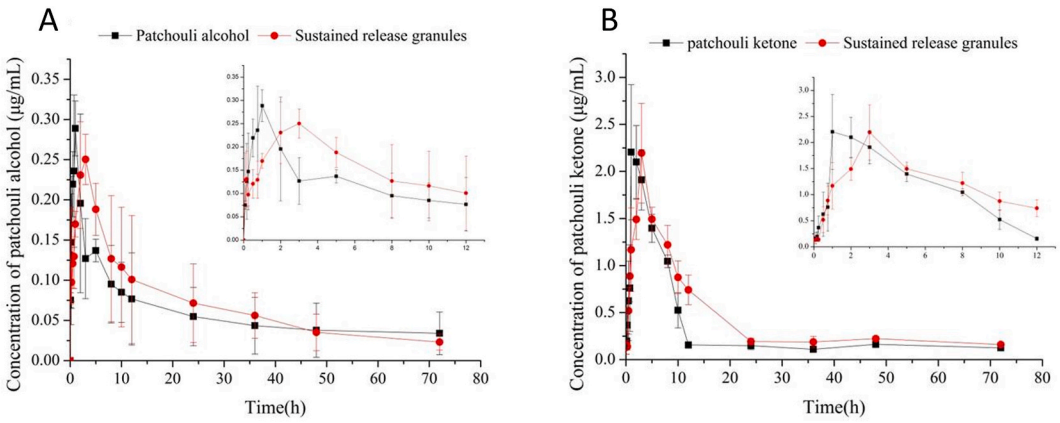

Fig. 7. Plasma concentration-time curves of patchouli alcohol(A) and patchouli ketone(B) in SD rats after oral administration (mean ± S.D, n = 6).

Table 2
Pharmacokinetic parameters of patchouli alcohol(a) and patchouli ketone(b) in SD rats after oral administration (mean ± S.D,n = 6).

Pharmacokinetic parameters	Powder group		Granule group	
	a	b	a	b
$AUC_{0\text{-}t}$, mg/L·h	4.658 ± 0.317	22.580 ± 0.226	5.466 ± 0.516*	29.700 ± 0.404*
$AUC_{0\text{-}\infty}$, mg/L·h	5.731 ± 0.292	24.347 ± 2.756	6.478 ± 0.489*	35.052 ± 2.683*
$MRT_{(0\text{-}t)}$, h	27.781 ± 2.016	18.081 ± 0.371	24.153 ± 1.635*	20.261 ± 0.361*
$MRT_{(0\text{-}\infty)}$, h	35.529 ± 2.930	33.993 ± 2.506	38.412 ± 6.778	36.565 ± 2.412
$t_{1/2}$, h	24.348 ± 2.985	26.804 ± 2.745	28.199 ± 6.213	27.372 ± 0.491
T_{max}, h	0.958 ± 0.093	1.000 ± 0.000	3.000 ± 0.000*	2.983 ± 0.037*
C_{max}, mg/L	0.301 ± 0.013	2.295 ± 0.050	0.257 ± 0.017*	2.125 ± 0.050*

*$P < 0.05$, versus the powder group.

are essential for enhancing the therapeutic efficacy of oils against *H. pylori*. The combination of EC and HPMC contributed to a controlled and sustained release of PO, thereby increasing its bioavailability.

Utilizing CSD as an adsorbent and floating agent introduces a novel strategy in gastro-retentive drug delivery systems. Its ability to absorb large amounts of oil without affecting the powder's flow properties is a considerable advantage.

Our *in vitro* and *in vivo* experiments confirm the superiority of the formulated granules. However, to establish the clinical viability of this system, future studies should concentrate on evaluating its long-term stability and conducting trials to access its biocompatibility and therapeutic efficacy in animal models and ultimately in human subjects.

CRediT authorship contribution statement

Chen Liu: Writing – original draft, Methodology, Funding acquisition, Formal analysis. **Yanan Wu:** Writing – original draft, Methodology. **Yeli Zou:** Methodology, Formal analysis. **Jiao Wang:** Formal analysis. **Boli Li:** Methodology, Formal analysis. **Yanni Ma:** Methodology, Formal analysis. **Xia Zhang:** Methodology, Formal analysis. **Wenping Wang:** Writing – review & editing, Funding acquisition, Conceptualization.

Ethical statement

The animal study protocol was approved by the Institutional Ethics Committee of Ningxia Medical University (protocol code 2016-046 and date of approval March 10, 2016).

Funding

This work was supported by the National Natural Science Foundation of China (No. 81660665, 81760713, 81960719), and the Reserve Talents Project for Young and Middle-Aged Academic and Technical Leaders in Yunnan Province (grant no. 202205AC160038).

Declaration of competing interest

The authors declare that they have no known competing financial interests or personal relationships that could have appeared to

influence the work reported in this paper.

References

[1] G. Hu, C. Peng, X. Xie, S. Zhang, X. Cao, Availability, pharmaceutics, security, pharmacokinetics, and pharmacological activities of patchouli alcohol, Evid Based Complement Alternat Med 2017 (2017) 4850612.
[2] C. Junren, X. Xiaofang, L. Mengting, X. Qiuyun, L. Gangmin, Z. Huiqiong, C. Guanru, X. Xin, Y. Yanpeng, P. Fu, P. Cheng, Pharmacological activities and mechanisms of action of Pogostemon cablin Benth: a review, Chin. Med. 16 (1) (2021) 5.
[3] F. Xu, W. Cai, T. Ma, H. Zeng, X. Kuang, W. Chen, B. Liu, Traditional uses, phytochemistry, pharmacology, quality control, industrial application, pharmacokinetics and network pharmacology of Pogostemon cablin: a comprehensive review, Am. J. Chin. Med. 50 (3) (2022) 691–721.
[4] D.W. Lian, Y.F. Xu, Q.H. Deng, X.M. Lin, B. Huang, S.X. Xian, P. Huang, Effect of patchouli alcohol on macrophage mediated Helicobacter pylori digestion based on intracellular urease inhibition, Phytomedicine 65 (2019) 153097.
[5] Y. Xu, Q. Deng, Y. Zhong, L. Jing, H. Li, J. Li, H. Yu, H. Pan, S. Guo, H. Cao, P. Huang, B. Huang, Clinical strains of Helicobacter pylori with strong cell invasiveness and the protective effect of patchouli alcohol by improving miR-30b/C mediated xenophagy, Front. Pharmacol. 12 (2021) 666903.
[6] W. Leong, G. Huang, I. Khan, W. Xia, Y. Li, Y. Liu, X. Li, R. Han, Z. Su, W.L.W. Hsiao, Patchouli essential oil and its derived compounds revealed prebiotic-like effects in C57BL/6J mice, Front. Pharmacol. 10 (2019) 1229.
[7] J. Baj, A. Forma, M. Sitarz, P. Portincasa, G. Garruti, D. Krasowska, R. Maciejewski, Helicobacter pylori virulence factors-mechanisms of bacterial pathogenicity in the gastric microenvironment, Cells 10 (1) (2020).
[8] A. O'Connor, T. Furuta, J.P. Gisbert, C. O'Morain, Review - treatment of Helicobacter pylori infection 2020, Helicobacter 25 (Suppl 1) (2020) e12743.
[9] T. Kakiuchi, K. Yamamoto, I. Imamura, K. Hashiguchi, H. Kawakubo, D. Yamaguchi, Y. Fujioka, M. Okuda, Gut microbiota changes related to Helicobacter pylori eradication with vonoprazan containing triple therapy among adolescents: a prospective multicenter study, Sci. Rep. 11 (1) (2021) 755.
[10] M. Ruiz-Rico, Y. Moreno, J.M. Barat, In vitro antimicrobial activity of immobilised essential oil components against Helicobacter pylori, World J. Microbiol. Biotechnol. 36 (1) (2019) 3.
[11] H.A. Alomar, N. Fathallah, M.M. Abdel-Aziz, T.A. Ibrahim, W.M. Elkady, GC-MS profiling, anti-Helicobacter pylori, and anti-inflammatory activities of three apiaceous fruits' essential oils, Plants 11 (19) (2022).
[12] E. Al-Sayed, H.A. Gad, D.M. El-Kersh, Characterization of four piper essential oils (GC/MS and ATR-IR) coupled to chemometrics and their anti-Helicobacter pylori activity, ACS Omega 6 (39) (2021) 25652–25663.
[13] M. Uboldi, A. Melocchi, S. Moutaharrik, L. Palugan, M. Cerea, A. Foppoli, A. Maroni, A. Gazzaniga, L. Zema, Administration strategies and smart devices for drug release in specific sites of the upper GI tract, J Control Release 348 (2022) 537–552.
[14] S. Dhiman, N. Philip, T. Gurjeet Singh, R. Babbar, N. Garg, V. Diwan, P. Singh, An insight on novel approaches & perspectives for gastro-retentive drug delivery systems, Curr. Drug Deliv. 20 (6) (2023) 708–729.
[15] R. Grosso, M.V. de-Paz, Scope and limitations of current antibiotic therapies against Helicobacter pylori: reviewing amoxicillin gastroretentive formulations, Pharmaceutics 14 (7) (2022).
[16] S. He, K. Li, C. Du, Z. Li, Y. Huang, C. Cao, Temperature and pH dual response flexible silica aerogel with switchable wettability for selective oil/water separation, Mar. Pollut. Bull. 199 (2024) 116011.
[17] N. Morgulchik, N. Kamaly, Meta-analysis of in vitro drug-release parameters reveals predictable and robust kinetics for redox-responsive drug-conjugated therapeutic nanogels, ACS Appl. Nano Mater. 4 (2021).
[18] R.B. Kjeldsen, M.N. Kristensen, C. Gundlach, L.H.E. Thamdrup, A. Müllertz, T. Rades, L.H. Nielsen, K. Zór, A. Boisen, X-Ray imaging for gastrointestinal tracking of microscale oral drug delivery devices, ACS Biomater. Sci. Eng. 7 (6) (2021) 2538–2547.
[19] M. Rahamathulla, S. Saisivam, A. Alshetaili, U. Hani, H.V. Gangadharappa, S. Alshehri, M.M. Ghoneim, F. Shakeel, Design and evaluation of losartan potassium effervescent floating matrix tablets: in vivo X-ray imaging and pharmacokinetic studies in albino rabbits, Polymers 13 (20) (2021).
[20] V. Priya, Mehata AK. Vikas, D. Jain, S.K. Singh, M.S. Muthu, Efficient delivery of abciximab using mesoporous silica nanoparticles: in-vitro assessment for targeted and improved antithrombotic activity, Colloids Surf. B Biointerfaces 218 (2022) 112697.
[21] W. Chen, B. Yu, X. Zhang, F. Zhang, X. Zan, T. Li, Precisely controlling the surface roughness of silica nanoparticles for enhanced functionalities and applications, J. Colloid Interface Sci. 629 (Pt A) (2023) 173–181.
[22] D. Blanco, O. Antikainen, H. Räikkönen, J. Yliruusi, A.M. Juppo, Effect of colloidal silicon dioxide and moisture on powder flow properties: predicting in-process performance using image-based analysis, Int. J. Pharm. 597 (2021) 120344.
[23] D.J. Lunter, Evaluation of mesoporous silica particles as drug carriers in hydrogels, Pharmaceut. Dev. Technol. 23 (8) (2018) 826–831.
[24] M.A. Molaei, K. Osouli-Bostanabad, K. Adibkia, J. Shokri, S. Asnaashari, Y. Javadzadeh, Enhancement of ketoconazole dissolution rate by the liquisolid technique, Acta Pharm. 68 (3) (2018) 325–336.
[25] F. Xu, Q. Yang, L. Wu, R. Qi, Y. Wu, Y. Li, L. Tang, D.A. Guo, B. Liu, Investigation of inclusion complex of patchouli alcohol with β-cyclodextrin, PLoS One 12 (1) (2017) e0169578.
[26] J. He, H. Zhao, X. Li, D. Su, F. Zhang, H. Ji, R. Liu, Superelastic and superhydrophobic bacterial cellulose/silica aerogels with hierarchical cellular structure for oil absorption and recovery, J. Hazard Mater. 346 (2018) 199–207.
[27] M.M.A. Elsayed, M.O. Aboelez, M.S. Mohamed, R.A. Mahmoud, A.A. El-Shenawy, E.A. Mahmoud, A.A. Al-Karmalawy, E.Y. Santali, S. Alshehri, M.E.M. Elsadek, M.A. El Hamd, A.E.H. Ramadan, Tailoring of rosuvastatin calcium and atenolol bilayer tablets for the management of hyperlipidemia associated with hypertension: a preclinical study, Pharmaceutics 14 (8) (2022).
[28] A. Berardi, Rahim S. Abdel, L. Bisharat, M. Cespi, Swelling of zein matrix tablets benchmarked against HPMC and Ethylcellulose: challenging the matrix performance by the addition of Co-excipients, Pharmaceutics 11 (10) (2019).
[29] A.Y. Chaerunisaa, R. Ali, A. Dashevskiy, Release adjustment of two drugs with different solubility combined in a matrix tablet, AAPS PharmSciTech 20 (4) (2019) 142.
[30] D. Tsunashima, K. Yamashita, K.I. Ogawara, K. Sako, T. Hakomori, K. Higaki, Development of extended-release solid dispersion granules of tacrolimus: evaluation of release mechanism and human oral bioavailability, J. Pharm. Pharmacol. 69 (12) (2017) 1697–1706.
[31] H.S. Kim, C.M. Kim, A.N. Jo, J.E. Kim, Studies on preformulation and formulation of JIN-001 liquisolid tablet with enhanced solubility, Pharmaceuticals 15 (4) (2022).
[32] S. Ghumman, S. Noreen, H. Hameed, M. Elsherif, R. Shabbir, M. Rana, K. Junaid, Bukhari Apdsna, Synthesis of pH-sensitive cross-linked basil seed gum/acrylic acid hydrogels by free radical copolymerization technique for sustained delivery of captopril, Gels 8 (2022) 291.
[33] I.Y. Wu, S. Bala, N. Škalko-Basnet, M.P. di Cagno, Interpreting non-linear drug diffusion data: utilizing Korsmeyer-Peppas model to study drug release from liposomes, Eur. J. Pharmaceut. Sci. 138 (2019) 105026.
[34] B. Cheng, D. Li, Q. Huo, Q. Zhao, Q. Lan, M. Cui, W. Pan, X. Yang, Two kinds of ketoprofen enteric gel beads (CA and CS-SA) using biopolymer alginate, Asian J. Pharm. Sci. 13 (2) (2018) 120–130.
[35] R. Zhang, P. Yan, Y. Li, L. Xiong, X. Gong, C. Peng, A pharmacokinetic study of patchouli alcohol after a single oral administration of patchouli alcohol or patchouli oil in rats, Eur. J. Drug Metab. Pharmacokinet. 41 (4) (2016) 441–448.